Testing the Activation Analysis for Fusion in OpenMC

Son Quang, Nicholas R. Brown, and G. Ivan Maldonado
Department of Nuclear Engineering, University of Tennessee, Knoxville, TN 37996
squang@vols.utk.edu

***Abstract*—OpenMC is a community-developed Monte Carlo neutron and photon transport simulation code. It can perform fission simulations such as fixed-source, k-eigenvalue, and subcritical multiplication calculations on models built using either a constructive solid geometry or CAD representation. To explore the use of OpenMC for fusion activation analysis, a detailed model of the Fusion Neutronics Science Facility (FNSF) was first developed for comparisons against an existing SERPENT model. A 90-degree model of FNSF in Standard-Triangle-Language (STL) CAD format was converted to Constructive Solid Geometry (CSG) using each code's built-in functions, and the geometries were validated by ensuring no cells overlapped and no particles were lost during simulations. The neutron fluxes were calculated and compared for multiple components close to the plasma. The results show differences mostly below 1% in fluxes and averaged 8% for activity and decay heat. The work described in this study tests the CAD-based geometry using the DagMC toolkit in OpenMC and compares the activation analysis of OpenMC to SERPENT code.**

Keywords: Activation, FNSF, Fusion, OpenMC, SERPENT

I. INTRODUCTION

OpenMC's activation analysis features were evaluated against SERPENT by comparing various components' activity, decay heat, and radionuclide inventory as a function of time. It was observed that the inventory of radionuclides in activated materials calculated by SERPENT tends to have fewer radionuclides than OpenMC. Nevertheless, the total activity and decay heat of specific components at various timesteps agreed within 3% or less for most components; the highest difference of roughly 10% in certain time steps is due to ignored depletion chains when the atomic density of an isotope is negligible in SERPENT. Activation analyses with OpenMC took less computational time to achieve a similar uncertainty relative to SERPENT. The work described in this study shows that OpenMC can be a reliable tool for the activation analysis of a fusion device.

A. Fusion Neutronic Science Facility

The Fusion Energy System Studies-Fusion Nuclear Science Facility (FESS-FNSF) was conceptualized as a fusion energy development pathway toward the first commercial power plant [1], a concept that has continued to evolve until recently. FNSF will be aggressively pushed into the fusion nuclear regime, providing a fully integrated fusion nuclear environment in conjunction with fully integrated fusion core components (blanket, divertor, heating/current drive, and diagnostics), near-core components (vacuum vessel, cryostat, toroidal field coils, poloidal field/central solenoid coils, maintenance and inspection equipment, hot cell, feed pipes, and transmission lines), and finally ex-core components (tritium extraction, heat exchanger, fluid clean up, plasma heating/current drive source, vacuum pump, etc. [2], as depicted in Fig. 1.

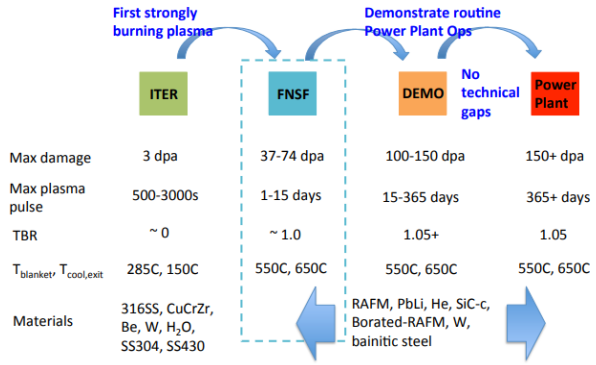

Fig. 1. Pathway to commercial fusion power illustrated along with several metrics describing how each facility incrementally approaches power plant parameters [2]

B. SERPENT

SERPENT [3] is a reactor physics neutronics and burnup calculation code developed at Finland's VTT Technical Research Centre since 2004. In recent years, however, the built-in capabilities have been extended to cover a broader scope of reactor physics applications, including the development of plasma sources and the implementation of CAD-based geometry from STL files [4].An activation analysis of FNSF activation assessments for inboard (IB) regions using SERPENT has been performed and compared to previous studies [5].

C. OpenMC

OpenMC is a community-developed Monte Carlo neutron and photon transport simulation code. The development of OpenMC was spearheaded by the Computational Reactor Physics Group (CRPG) at Massachusetts Institute of Technology (MIT) as part of a project to develop scalable parallel algorithms for future exascale supercomputers [6]. The code has been developed starting in 2011 and was first released to the public in December 2012. Relatively, OpenMC is quite a new particle transport code compared to other codes such as MCNP [7] or SERPENT [3]. In recent years, the development team has also grown to span multiple organizations [6]. Furthermore, many changes and features have been made that are very attractive to users, including powerful post-processing tools and modeling three-dimensional structured mesh. This study describes the application of OpenMC's modeling from the CAD model and depletion module.

II. METHODOLOGY

A. Geometry configurations

The FNSF model herein employed is a tokamak-based facility with a 518 MW fusion power, a plant Lifetime of 24 years (8.5 FPY), and 35 percent availability. At the first wall, the machine's average neutron wall loading (NWL) is estimated to be 1.1 MW/m2 [8]. CAD models were available to us from the Fusion Energy Science – Fusion Neutronics Science Facility design team. Fig. 2, shows side view of the FNSF model. The geometry shown is a 90-degree model built by duplicating 22.5-degree sectors.

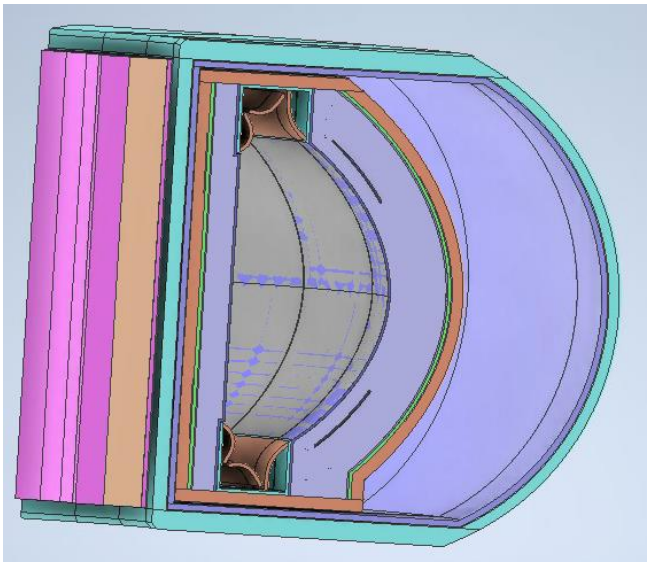

Fig. 2 Side view of the FNSF Model

SERPENT has a built-in feature that can read STL data format. The STL format consists of triangular facets that illustrate the outer boundary of each solid body. Each triangle consists of 3 vertices and 1 normal that defines the orientation and determines the inside and outside of the triangle.

Despite many advantages of the STL format, one may question the discretization errors of triangulation [9] because triangular facets are only approximations of surfaces, and curved surfaces can be underestimated or overestimated, *Fig. 3*.

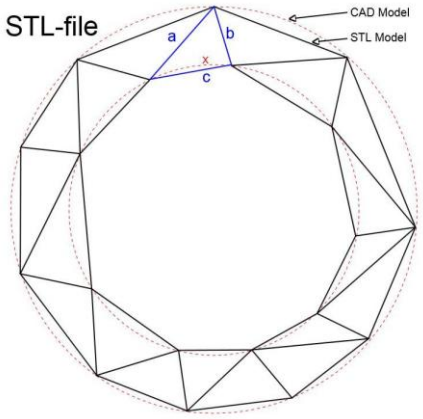

Fig. 3. STL approximation of a CAD torus

In the FNSF design, many components are very close to each other; thus, the overestimation of the triangulation can cause overlap between components. Fortunately, the user has control over the resolution of the triangular surface mesh. In theory, there is no upper limit for the resolution of the mesh, and the higher resolution will accurately represent the solid body. Increasing the resolution will require more computer memory, and the calculations will take longer to complete. The CAD model of FNSF was converted to STL with high resolution to preserve the shape and volume of components and ensure that there is no overlap between components that cause particle loss. Using the test mode in SERPENT with *-checkstl <N> <M>* option that sample <N> random points in the geometry and start <M> random rays in random directions originating from each point. The purpose of each test is to determine whether the point being tested is located within or outside of the solid body. The first intersection of the ray and solid body determines if the ray enters or exits the solid body. If the scalar product of the ray and the normal vector of the triangular facet at the intersection yields a positive result, the ray is exiting the solid body. Therefore, the point being tested is inside of the solid body. On the other hand, the ray and the normal vector of the triangular facet yield a negative scalar product; the ray is entering the solid; thus, the point is outside of the solid[9]. If all rays yield the same results, the point is passed. As illustrated in Fig. 4b, the STL files are appropriately constructed and have very high resolution; the pass rate is 100%.

On the other hand, OpenMC relies on the Direct Accelerated Geometry Monte Carlo (DAGMC) to represent CAD-based geometry in a surface mesh format for consistency in comparison. The STL files can be converted to DAGMC h5m format using the stl_to_h5m package **Error! Reference source not found.**. The maximum number of particles lost is set to 1, so if any particle is lost, the simulation is terminated. The cross-sectional view of the geometry in CAD, STL, SERPENT, and OpenMC are in Fig.4. The boundaries on the x and y axes are reflective boundary conditions, and the upper and lower planes have vacuum boundary conditions.

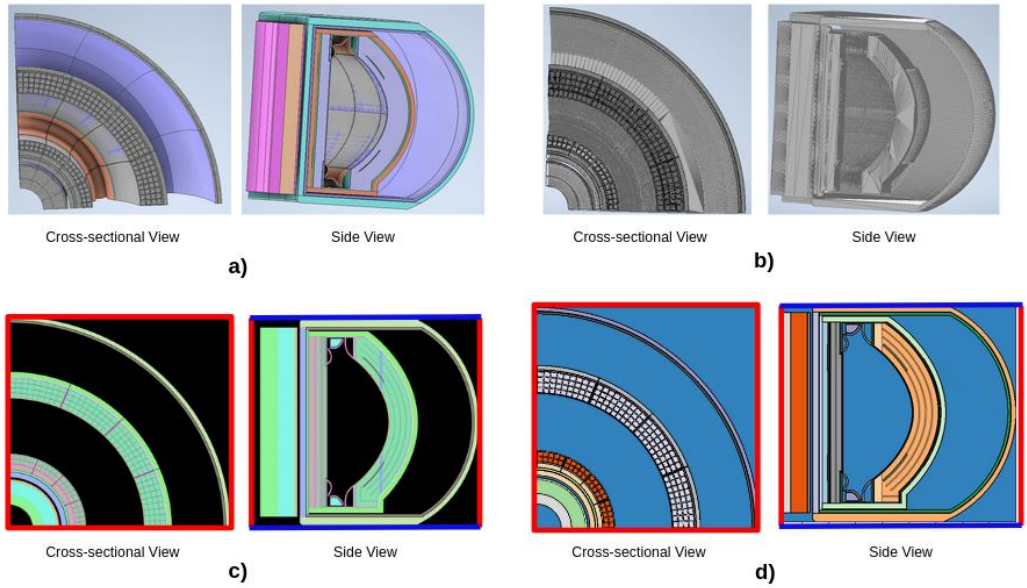

Fig. 4 Cross-sectional and side view of geometry. a) CAD, b) STL, c) plotted in SERPENT, d) plotted in OpenMC. Reflective boundary condition represented by red, vacuum boundary condition represented by blue.

B. *Simulation configuration*

1) Materials

The results heavily depend upon the specific materials and mass/volume fractions in the specific model used, which has changed and evolved frequently since the inception of the FNSF. It is essential to point out that some specific details and design choices of the FNSF have evolved over time and have changed from those reported in past studies. The materials in this study were pre-set based on decisions made during previous studies such as ARIES-ACT2 [10]. The material descriptions are the same as in the previous activation study using SERPENT [5].

2) Neutron Source

There are sub-routines to describe the distribution of the plasma source in SERPENT and pre-built neutron source packages for fusion application in OpenMC. However, for consistency between the two codes, the neutron source used in this study is 14.1 MeV with 3 nested regions with 63%, 32%, and 5% corresponding source strength distributions, as shown in Fig. 5.

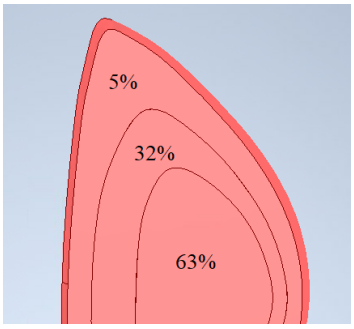

Fig. 5 Neutron source distribution

3) Cross section library

This model utilizes the TENDL-2017 **Error! Reference source not found.** nuclear data library for cross section and ENDF/B-VIII [14]for decay data in both SERPENT and OpenMC.

III. RESULTS AND COMPARISON

The results from simulations are used to compare between two codes, including flux across components, activity, and decay heat of components after irradiation. Fig. 6 illustrates the mid-plane radial builds for the Inboard (IB) and Outboard (OB) of the FNSF from the CAD model. It is worth noting that the complex geometry of the FNSF with multiple shielding components causes a significant challenge with Monte Carlo calculation. Heavily shielded regions were evaluated with variance reduction to obtain reasonable statistics. The results show specific activity and decay heat that are several orders of magnitude lower than all other components. For ease of display of data, these results are not included for heavily shielded regions.

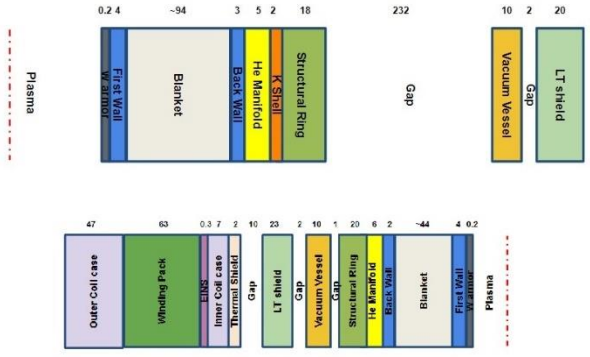

Fig. 6. Outboard (top) and Inboard (bottom) radial builds.

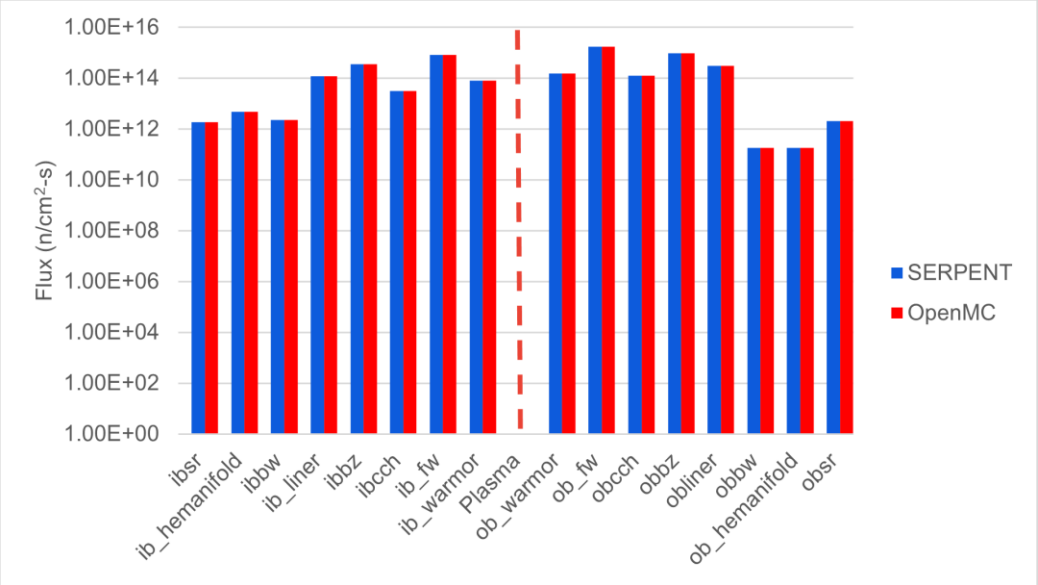

Fig. 7. Calculated fluxes of various components in SERPENT and OpenMC.

The components close to the plasma including: IB and OB tungsten armor (ib_warmor, ob_warmor), IB and OB first wall (ib_fw, ob_fw), IB and OB blanket cooling channel (ibcch, obcch), IB and OB blanket breeding zone (ibbz, obbz), IB and OB blanket liner (ib_liner, ob_liner), IB and OB backwall (ib_bw, ob_bw), IB and OB helium manifold (ib_hemanifold, ob_hemanifold), IB and OB structural ring (ibsr, obsr).

A. Flux comparison.

The flux in components is scored using materials detectors. OpenMC used MaterialFilter to score the event in materials. The equivalent in SERPENT is detector with a 'dm' card. The unit of flux in SERPENT is [particles/cm^{2}s]. Meanwhile, OpenMC returns flux in the unit of [particle.cm/source particle]; thus, the OpenMC must be converted to the same unit as SERPENT results. The OpenMC flux is converted using Eq. 1.

$$[OpenMC\ flux] \times {}^{S}/_{V} \qquad (1)$$

With:
S: source strength (particles/s)
V: volume of cell (cm^3)

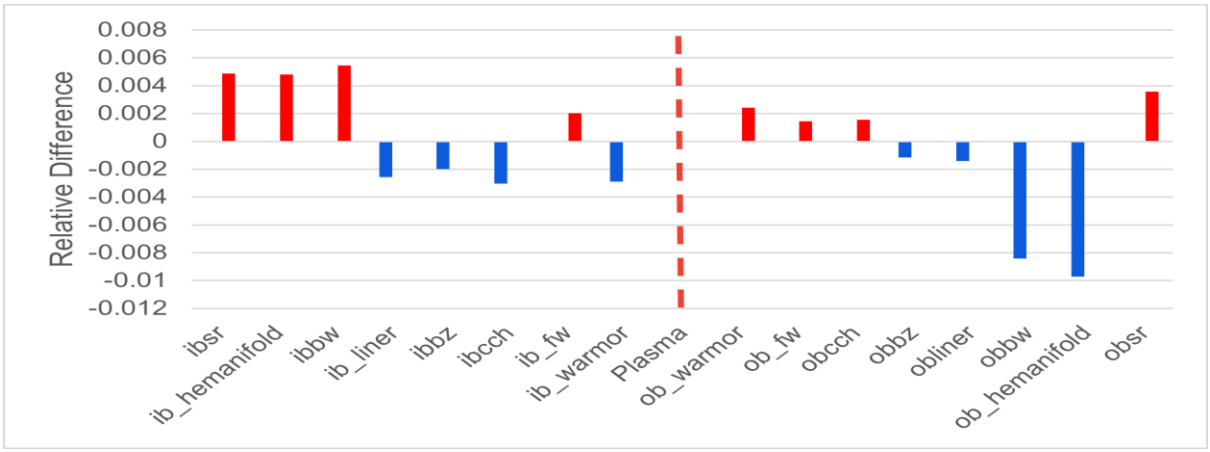

Fig. 8. The relative difference of neutron fluxes between SERPENT and OpenMC, negative differences presented by blue, and positive differences presented by red.

The results of calculated neutron fluxes are compared in Fig 7, and the relative difference of neutron fluxes between SERPENT and OpenMC is presented in Fig. *8*. The relative difference between SERPENT and OpenMC is calculated using Eq. 2.

$$\frac{OpenMC-SERPENT}{SERPENT} \quad (2)$$

The neutron fluxes at various components of interest show good agreement between OpenMC and SERPENT calculation. The most significant relative difference is approximately 1%.

B. Decay Activity

The assumption used in this study is that the irradiation time for all components assumes the plant's lifetime of 8.5 full power years (FPY). However, some components, such as the tungsten armor (W Armor) and first wall (FW), are expected to have shorter irradiation periods due to radiation damage and would be replaced every few years [15]. Our simulation assumes that the W Armor and FW are irradiated during the entire plant's lifetime (8.5 FPY), which is a conservative estimation.

The transmutation of nuclides by nuclear reactions and radioactive decay inside an irradiated environment can be compactly described in matrix form Eq. 3[16].

$$\frac{d\boldsymbol{n}}{dt} = \boldsymbol{A}(\boldsymbol{n}, t)\boldsymbol{n}, \qquad \boldsymbol{n}(0) = \boldsymbol{n}_0$$

where

$$\boldsymbol{n} = \begin{pmatrix} N_1 \\ N_2 \\ \vdots \\ N_n \end{pmatrix}, \quad \boldsymbol{n}_0 = \begin{pmatrix} N_{1,0} \\ N_{2,0} \\ \vdots \\ N_{n,0} \end{pmatrix} \quad (3)$$

A(n,t) is the burnup matrix containing the decay and transmutation coefficients

To solve for the burnup matrices at various time, both codes use the Chebyshev rational approximation method (CRAM) to evaluate matrix exponentials, although the way in which OpenMC and SERPENT implement these methods are different[6][16][17][19].

OpenMC is currently implementing the incomplete partial fraction (IPF) CRAM [16][19]. The matrix exponential is approximated as Eq. 4[20]:

$$\hat{r}_{k,k}(\boldsymbol{A}t)\boldsymbol{n}_0 = \alpha_0 \prod_{j=1}^{k/2} \left(\boldsymbol{I} + 2Re\left\{\alpha_j \left(\boldsymbol{A}t - \theta_j \boldsymbol{I}\right)^{-1}\right\}\right)\boldsymbol{n}_0 \quad (4)$$

Meanwhile, the approach used by SERPENT is based on the partial fraction decomposition form (PFD) CRAM; the solution can be written as Eq. 5[18]:

$$\hat{r}_{k,k}(\boldsymbol{A}t)\boldsymbol{n}_0 = \alpha_0 \boldsymbol{n}_0 \; + 2Re\left(\sum_{j=1}^{k/2} \alpha_j \left(\boldsymbol{A}t - \theta_j \boldsymbol{I}\right)^{-1} \boldsymbol{n}_0\right) \quad (5)$$

Where k is the order of the approximation, and α_0, α_j, and θ_j are the corresponding coefficients in k^{th} order. The simulations used the default order of approximations for CRAM in SERPENT and OpenMC, k=14 and k=48, respectively. PFD is considered one of the most popular forms for computing rational matrix functions because of computational time efficiency. However, the magnitude of the residues (α_l) will increase as the degree of the approximation increases [18]. This increases the susceptibility of the approximation to round-off mistakes. Compared to PFD, IPF provides a good balance of numerical stability and efficiency [16] because the IPF is expected to be less sensitive to round-off errors[18].

The transmutation chains are formed automatically in SERPENT. Meanwhile, the user will have to create a depletion chain. For this work, the depletion chain for OpenMC was formed with all available isotopes in the ENDF/B-VIII library [14].

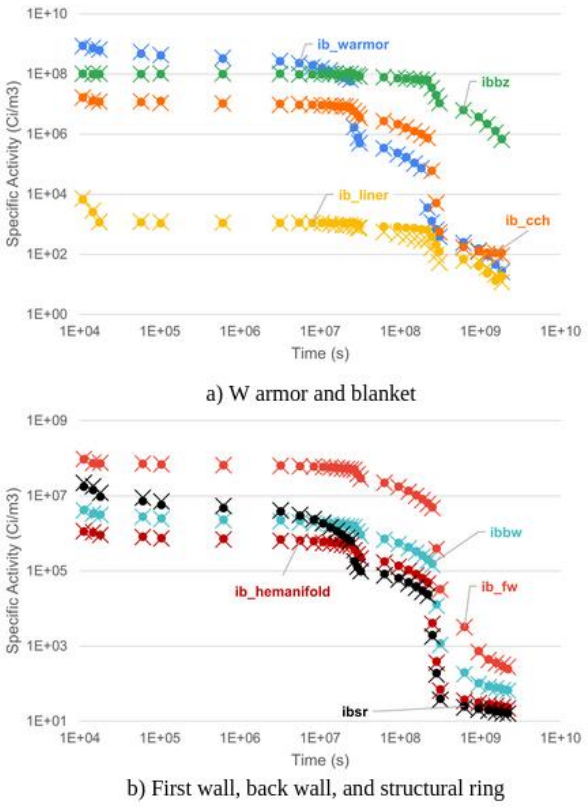

Fig. 9 Specific decay activity of IB components from OpenMC (•) and SERPENT (×).

The activity of material in OpenMC is extracted using the *get_activity()* function. SERPENT depletion results from SERPENT's MATLAB output are parsed using the serpentTools [21] python package. Fig. 9 presents the specific decay activity over time of IB components, and Fig. 10 presents the OB components.

Figure. 9 and Fig. 10 show a good agreement between decay activity calculations done in SERPENT and OpenMC. To accurately track all possible radioisotopes, both OpenMC and SERPENT will track all the decay paths that are available in the ENDF/B-VIII decay library. However, in SERPENT, the chain will be ignored when the atomic density of the isotope is less than 10^{-28} fraction of the total atomic density. Meanwhile, OpenMC will follow the chain until the atomic density of an isotope is 0. Thus, in Fig. 9a and Fig. 10a, the specific activity of the IB and OB liner calculated by OpenMC is significantly higher than SERPENT results, roughly 10%.

C. Decay heat

Decay heat and activity are direct outputs of SERPENT simulation, while decay heat calculation capability was only added into OpenMC recently in version *0.13.3*. OpenMC uses the *get_decay_heat()* method to calculate the decay heat of materials based on the nuclide's atom densities in the material with corresponding decay energy, decay constant from the decay library. The result of decay heat for various components calculated by SERPENT and OpenMC is presented in Fig. 11 and Fig. 12.

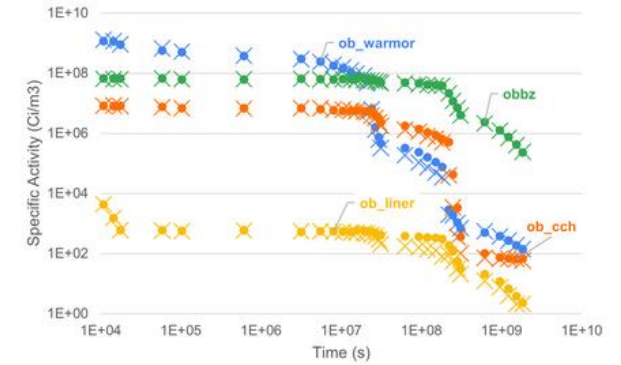

a) W armor and blanket

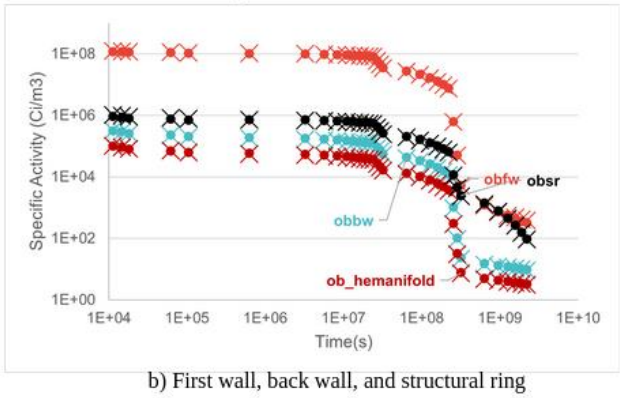

b) First wall, back wall, and structural ring

Fig. 11 Specific decay activity of OB components from OpenMC (•) and SERPENT (×).

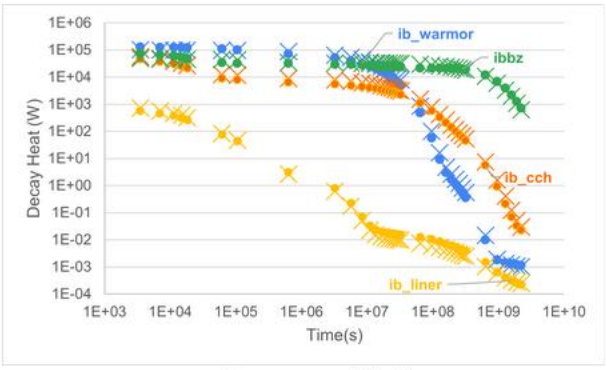

a) W armor and blanket

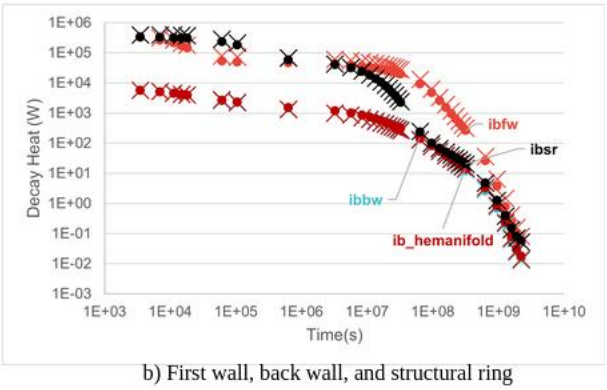

b) First wall, back wall, and structural ring

Fig. 10 Decay heat of IB components from OpenMC (•) and SERPENT (×).

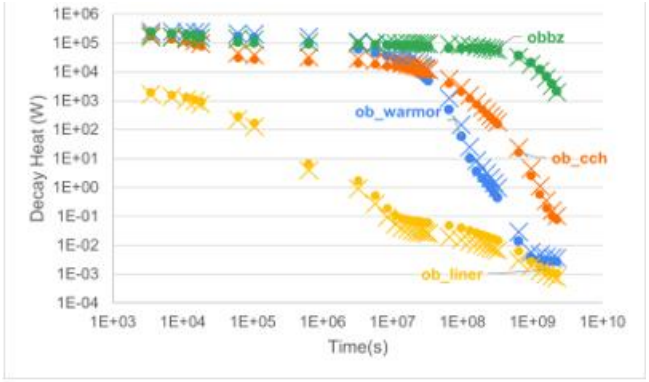

a) W armor and blanket

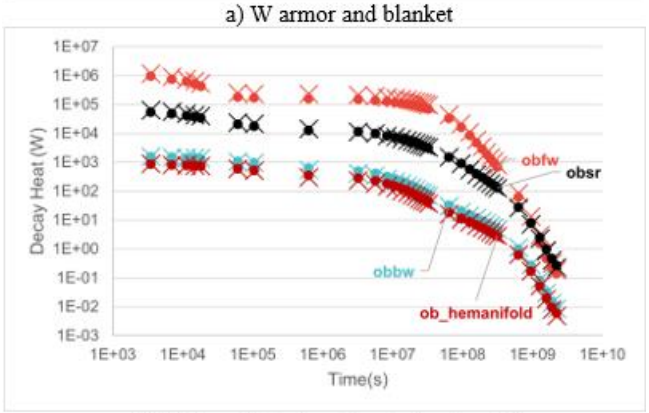

b) First wall, back wall and structural ring

Fig. 12 Decay heat of OB components from OpenMC (•) and SERPENT (×).

The decay heat results from OpenMC show a good agreement with the decay heat calculated by SERPENT.

IV. Conclusion

OpenMC is a Monte Carlo transport code with features that are attractive to users. OpenMC can perform simulations with CAD geometry using DAGMC to generate a mesh, which is very useful for simulations with detailed and complex geometry. The capabilities to perform post-irradiation and activation were just added in recent versions. The results here using *get_activity()* and *get_decay_heat()* methods to calculate activity and decay heat.

The work presented compares the simulation using CAD geometry with SERPENT and OpenMC using the FNSF model. The FNSF geometry was derived from STL format, which can be read directly by SERPENT. Meanwhile, OpenMC relies on DAGMC to convert STL files to the format that OpenMC can read. The geometry was checked in both codes to ensure there was no overlap that could affect the accuracy of conversion. In comparison, the calculated flux across various components in OpenMC and SERPENT agreed within 1% difference. The activity and decay heat of materials were calculated using decay data from ENDF/B-VIII, and the results for most materials agreed within 3%. Except for the IB and OB liner, where the OpenMC result is roughly 10% higher than the results calculated by SERPENT. The differences could be related to some depletion chains in SERPENT that were neglected due to insignificant atom densities.

Acknowledgment

The authors acknowledge the support from the US Department of Energy, Office of Fusion Energy Sciences under contract No.DE-SC0022308

I would like to express sincere thanks to Dr. Jiankai Yu, who is currently a research scientist at Center of Nuclear Energy Systems, for creating the code for *get_decay_heat()* method and helping us with OpenMC. I am also grateful to Dr. Felipe S.

Novais, who is currently a post-doc at MIT, for helping with CAD geometry usage in OpenMC.

REFERENCES

[1] C. E. Kessel, et al., "The Fusion Nuclear Science Facility, the Critical Step in the Pathway to Fusion Energy," Fusion Science and Technology, 68, 2, 225–236 (2015).

[2] C. E. Kessel, et al., "Overview of the fusion nuclear science facility, a credible break-in step on the path to fusion energy". Fusion Engineering and Design, 2018. 135: p. 236-270 (2017).

[3] J. Leppänen., et al. "The Serpent Monte Carlo code: Status, development and applications in 2013." Ann. Nucl. Energy, 82 (2015) 142-150.

[4] J. Leppänen and T. Kaltiaisenaho "Expanding the Use of Serpent 2 to Fusion Applications: Shut-down Dose Rate Calculations." PHYSOR 2016. Sun Valley, ID (2016).

[5] Son N. Quang, Jonathan Wing, Nicholas R. Brown & G. Ivan Maldonado (2023): Activation Analysis for the Inboard Region of FNSF Using SERPENT, Fusion Science and Technology, DOI: 10.1080/15361055.2023.2185043

[6] Paul K. Romano, Nicholas E. Horelik, Bryan R. Herman, Adam G. Nelson, Benoit Forget, and Kord Smith, "OpenMC: A State-of-the-Art Monte Carlo Code for Research and Development," Ann. Nucl. Energy, 82, 90–97 (2015).

[7] C. J. Werner (editor), "MCNP users manual - code version 6.2," LA-UR-17-29981, 2017.

[8] A. Davis., et al. "Neutronics aspects of the FESS-FNSF." Fusion Engineering and Design 135: 271-278 (2018).

[9] J. Leppänen, Methodology, applications and performance of the CAD-based geometry type in the serpent 2 Monte Carlo code, Annals of Nuclear Energy, Volume 176, 2022, 109259, ISSN 0306-4549, https://doi.org/10.1016/j.anucene.2022.109259.

[10] Shimwell, J., & Shriwise, P. Stl-to-5m: Convert non-overlapping STL files into a DAGMC h5m file complete with material tags and ready for use in neutronics simulations. (Version 0.2.3) [Computer software]. https://github.com/fusion-energy/stl_to_h5m.

[11] L. El-Guebaly and L. Mynsberge, "Neutronics characteristics, shielding system, activation, and environmental aspects of ARIES-ACT-2 power plant," University of Wisconsin, Fusion Technology Institute Report, UWFDM-1418, Dec. 2014. Available at: https://fti.neep.wisc.edu/fti.neep.wisc.edu/pdf/fdm1418.pdf.

[12] S. Smolentsev, "MHD thermohydraulics analysis and supporting R&D for DCLL blanket in the FNSF", Fusion Engineering and Design, 135, Part B,2018, 314-323 (2017); https://doi.org/10.1016/j.fusengdes.2017.06.017.

[13] A.J. Koning, D. Rochman, J. Sublet, N. Dzysiuk, M. Fleming and S. van der Marck, "TENDL: Complete Nuclear Data Library for Innovative Nuclear Science and Technology", Nuclear Data Sheets 155 (2019).

[14] Conlin, Jeremy Lloyd, Haeck, Wim, Neudecker, Denise, Parsons, Donald Kent, and White, Morgan Curtis. Release of ENDF/B-VIII.0-Based ACE Data Files. United States: N. p., 2018. Web. doi:10.2172/1438139.

[15] B. M. Madani and L. El-Guebaly, "Shielding and Activation Analyses for Inboard Region of FESS-FNSF Design," UWFDM-1423, University of Wisconsin Fusion Technology Institute Report, UWFDM-1423 (November 2015). Available at: https://fti.neep.wisc.edu/fti.neep.wisc.edu/pdf/fdm1423.pdf

[16] P. K. Romano et al. Depletion capabilities in the OpenMC Monte Carlo particle transport code. Annals of Nuclear Energy. 152 (2021) https://doi.org/10.1016/j.anucene.2020.107989

[17] Pusa, M., & Leppänen, J. (2010). Computing the Matrix Exponential in Burnup Calculations. Nuclear Science and Engineering, 164(2), 140-150. https://doi.org/10.13182/NSE09-14

[18] Pusa Maria (2016) Higher-Order Chebyshev Rational Approximation Method and Application to Burnup Equations, Nuclear Science and Engineering, 182:3, 297-318, DOI: 10.13182/NSE15-26

[19] E. E. Peterson et al. Development and validation of fully open-source R2S shutdown dose rate capabilities in OpenMC. Nuclear Fusion 64 (2024) https://doi.org/10.1088/1741-4326/ad32dd

[20] Binhang Zhang, XianBao Yuan, Yonghong Zhang, Haibo Tang, Liangzhi Cao, "Development of a versatile depletion code AMAC", Annals of Nuclear Energy, Volume 143, 2020, 107446, ISSN 0306-4549, https://doi.org/10.1016/j.anucene.2020.107446.

[21] Andrew Johnson, Dan Kotlyar, Stefano Terlizzi, and Gavin Ridley, "serpentTools: A Python Package for Expediting Analysis with Serpent," Nuc. Sci. Eng, (in press) (2020).